WILEY | Hindawi

Research Article

Thin-Film Nanocomposite Reverse Osmosis Membrane with High Flux and Antifouling Performance via Incorporating Maleic Anhydride-Grafted Graphene Oxide

Zhongyan Chen, Boqun Zhao, Yuhang Qin, Yi Zhou, Yinghua Lu, and Wenyao Shao (iD)

Department of Chemical and Biochemical Engineering, College of Chemistry and Chemical Engineering, Xiamen University, Xiamen 361005, China

Correspondence should be addressed to Wenyao Shao; wyshao@xmu.edu.cn

Water flux is one of the most important performance parameters of the reverse osmosis (RO) membrane. The higher water flux means lower energy cost when treating the same volume of feed solution with membrane separation technology. However, the increase of membrane water flux always corresponds to the decrease of solvent rejection, known as the "trade-off" effect. In addition, the surface fouling of membranes is often a serious problem, as frequent cleaning not only increases the operating cost but also shortens the life of the membranes. Recently, various hydrophilic nanomaterials have been used to improve the performance of membranes. To fabricate thin film nanocomposite (TFN) RO membrane with high flux and antifouling performance, maleic anhydride-grafted graphene oxide (MG) was successfully synthesized and incorporated into the polyamide (PA) layer via the interfacial polymerization (IP) method. We performed the IP reaction with m-phenylenediamine (MPD) and trimesoyl chloride (TMC) as reactive monomers on a polysulfone (PSF) substrate, and acid absorbent (TEA) and surfactant (SDS) were added to improve the separation performance of the membrane. The effects of MG incorporation on the membrane morphology and separation performance were investigated. SEM and AFM results show that the surface of the MG membrane is rougher than that of the membrane without MG. In addition, excessive loading of MG will lead to aggregation of MG nanosheets. FT-IR spectra indicate that the interaction between MG and PA layers results in an increase of hydrophilic groups on the surface of the TFN membrane, which is further confirmed by the results of the contact angle. The optimal MG doping concentration in the aqueous solution is 0.004 wt%, the water flux of the resultant TFN membrane is significantly increased to 51 $L \cdot m^{-2} \cdot h^{-1}$, 150% higher than the blank control membrane, which also performs a higher NaCl rejection (97.5% vs. 96.6%). Furthermore, the MG-incorporated RO membrane exhibits superior antifouling performance compared with the blank control membrane.

1. Introduction

With the development of industrialization and the increase of population, the demand for water resources is increasing. In addition, due to the unreasonable development and utilization of fresh water, the problem of water resources is becoming increasingly serious. The most effective way to solve this problem is to convert unusable water into usable water, such as seawater desalination or industrial wastewater treatment. RO membrane separation technology has been widely used in water treatment because of its high perfor-

mance, low cost, convenient operation, and low pollution [1–3]. However, the water flux and rejection of polyamide thin film composite (PA-TFC) membrane are mutually restricted. Increasing the membrane flux while maintaining high salt rejection has been the research focus of RO membrane separation technology [4–6]. In recent years, the rapid development of nanomaterials has brought a positive impact on polymer membrane materials. It is expected to solve the problem of the "trade-off" effect between water flux and membrane rejection [7]. Graphene oxide (GO) is a kind of two-dimensional nanomaterials with a special structure,
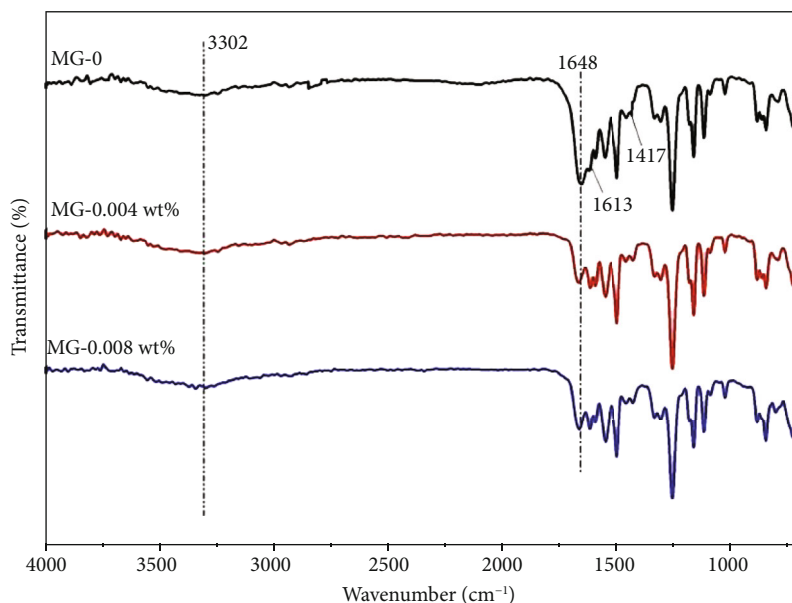
FIGURE 1: FT-IR spectra of composite membranes prepared with different MG concentrations.

which is widely used in membrane separation technology because of its strong hydrophilicity, good dispersion, high specific area, and reasonable pore structure.

In previous studies, graphene oxide has been widely used in membranes to improve their performances. In 2012, Wang et al. [8] dissolved polyvinylidene fluoride and graphene oxide into N,N-dimethylformamide, prepared a composite ultrafiltration (UF) membrane by phase conversion method, and studied its mechanical properties, permeability, and antifouling performance. Mi [9] found that adjusting the interlayer spacing of the graphene oxide membrane could achieve different separation goals. Sun et al. [10] designed a graphene oxide membrane with adjustable thickness; what is more, their research shows that changing the interlayer spacing of the graphene oxide membrane could improve the separation effect. Lu et al. [11] doped graphene oxide to the PA RO membrane and found that water flux and chlorine resistance increased, while salt retention was almost constant.

Further functionalization of the surface of graphene oxide is feasible, and the modified graphene oxide has more properties that enhance its application potential in the field of membrane technology. Maleic anhydride-grafted graphene oxide (MG) is a kind of graphene oxide whose surface is modified by maleic anhydride. Compared with GO, MG contains more active groups and its regularity is reduced. With the increase of interlayer spacing, the dispersion of MG in solution becomes better [12]. In this study, a series of MG-TFN membranes were prepared by incorporating MG into the active layer of the membranes via the interfacial polymerization method. The chemical composition, morphological characteristics, and hydrophilicity of MG-TFN membranes were tested by FTIR, SEM, AFM, and water contact angle characterization. The effects of MG incorporation on membrane separation performance and antifouling performance were investigated. This study proposes an idea for the preparation of high flux and antifouling RO membrane.
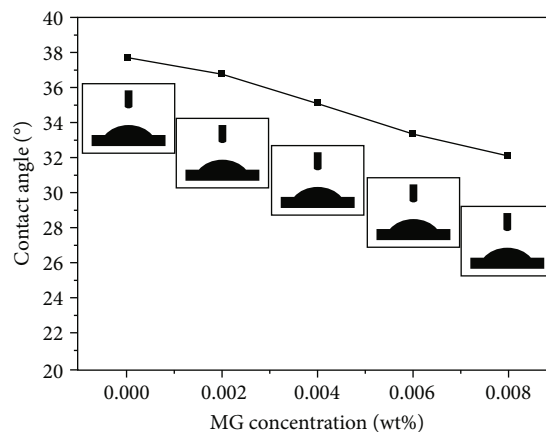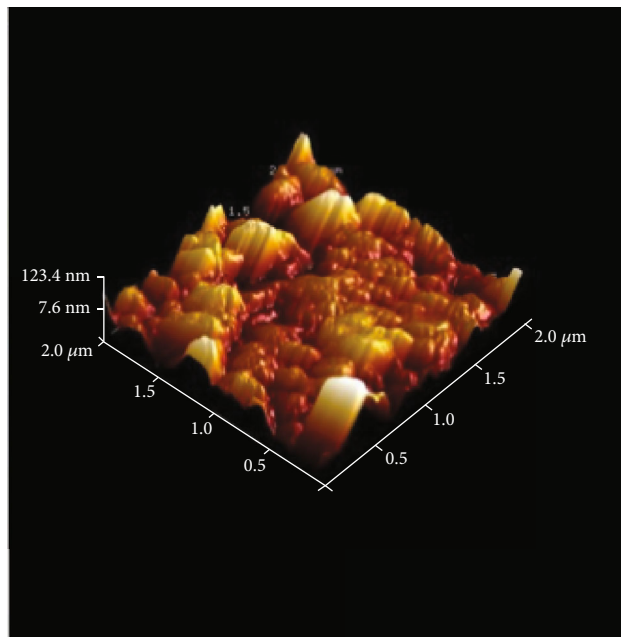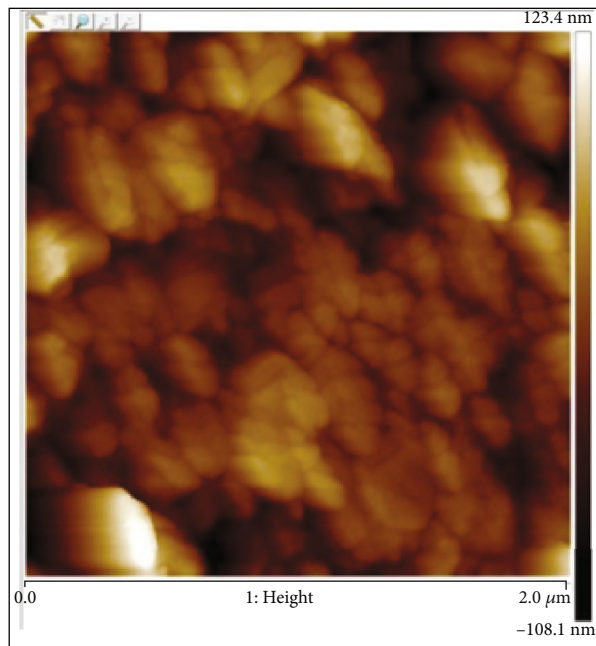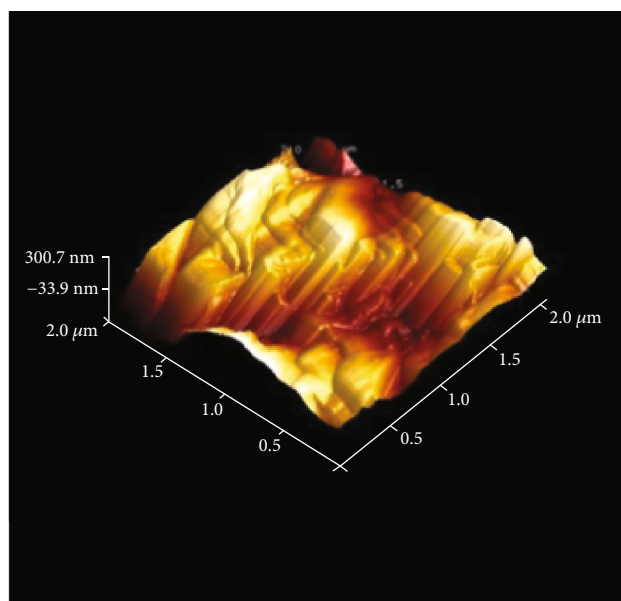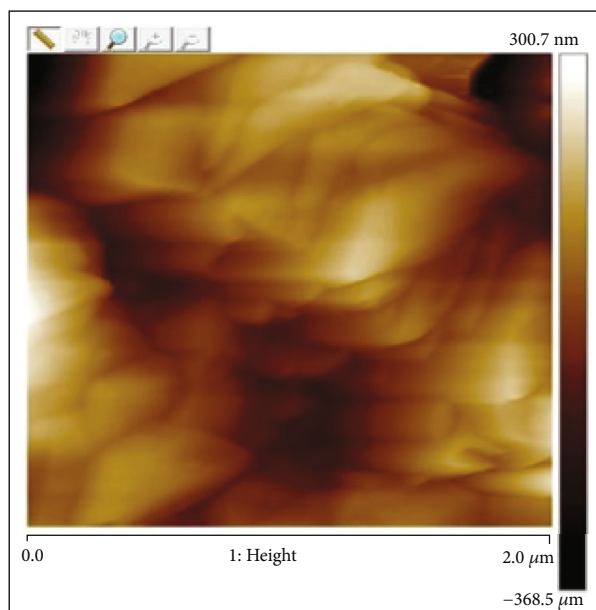

FIGURE 2: Contact angles of composite membranes prepared with different GO concentrations.

2. Experimental

2.1. Materials. A polysulfone (PSF) ultrafiltration membrane (Beijing Shengwanquan Xinli membrane Co., Ltd., China) was used as the support layer for interfacial polymerization. M-Phenylenediamine (MPD, Shanghai Macklin Biochemical Technology Co., Ltd., China) and trimesoyl chloride (TMC, Shanghai Macklin Biochemical Technology Co., Ltd., China) were used for fabricating the PA layer. Triethylamine (TEA, Sinopharm Chemical Reagent Co., Ltd., China) was used as the acid absorbent. Sodium lauryl sulfate (SDS, Xilong Chemical Co., Ltd., China) was used as the surfactant. N-Hexane (Sinopharm Chemical Reagent Co., Ltd., China) was used as the solvent. Sodium chloride (NaCl) was used for evaluating membrane performance. MG and ultrapure water were made in the laboratory.
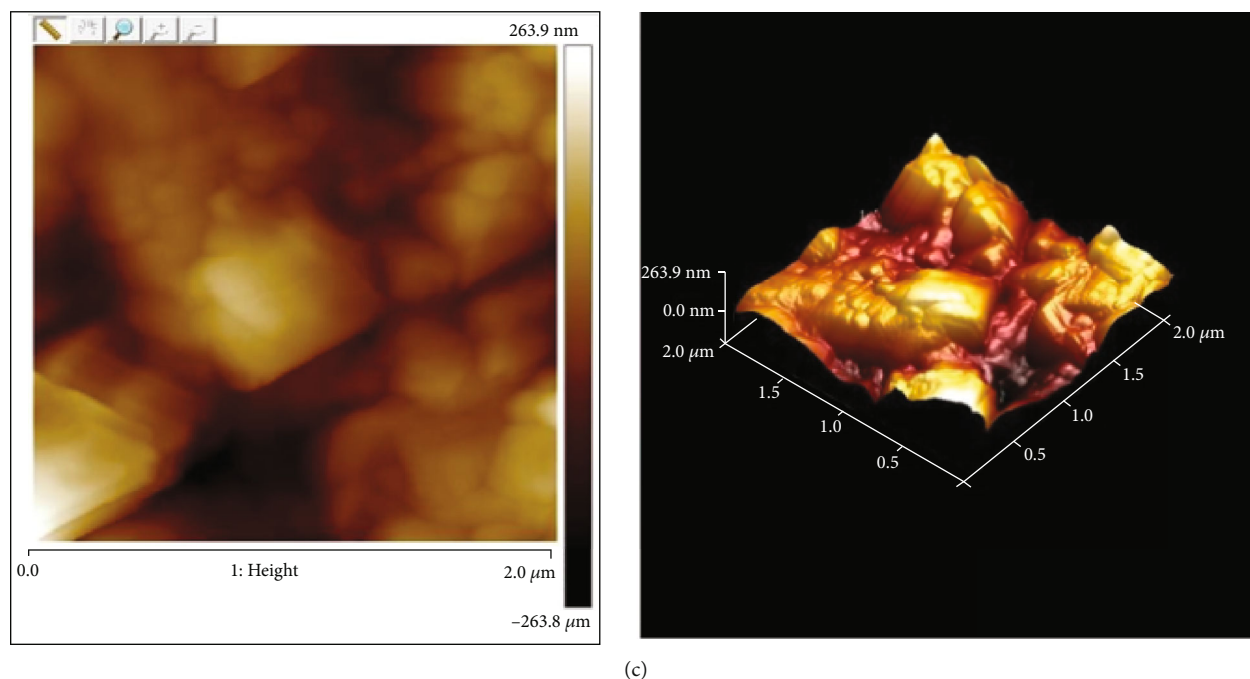
(a)

(b)

FIGURE 3: Continued.

(c)

FIGURE 3: AFM images of composite membranes prepared with different MG concentrations: (a) 0 wt%, (b) 0.004 wt%, and (c) 0.008 wt%.

2.2. Preparation of MG-TFN Membrane. The MG-TFN membrane was prepared by interfacial polymerization on the PSF UF membrane: the PSF UF membrane was immersed into a 2 wt% MPD, 2 wt% TEA, and 0.1 wt% SDS aqueous solution containing MG (0, 0.002, 0.004, 0.006, and 0.008 wt% of each) for 2 min. Excess MPD solution remaining on the PSF UF membrane was removed by flushing with nitrogen. After drying in air, the PSF UF membrane was immersed in 0.1 w/v% TMC in hexane for 1 min to form a PA layer via interfacial polymerization. Then, the membrane was dried in the vacuum oven at 60°C for 8 min and stabilized in pure water for 24 h. The TFN membrane that was made using a MPD solution containing x wt% of MG is denoted as the x-MG-TFN membrane.

2.3. Characterization of MG-TFN Membrane. The presence of MG in the prepared membrane was examined using a Fourier transform infrared (FTIR) spectrophotometer (VERTXE70, Bruker, Germany). The 0, 0.004, and 0.008-MG-TFN membranes were examined to analyze their molecular structure and chemical composition.

The contact angles were measured by a contact angle measurement instrument (SPCAX3, Beijing HARKE, China) to evaluate the hydrophilicity of the membrane. The membranes were dried for 24 h after preparation; then, the contact angles of the 0, 0.002, 0.004, 0.006, and 0.008-MG-TFN membranes were measured with a 3 μL DI water drop using the instrument. The contact time between the drop and the membrane surface of each sample was 30 s.
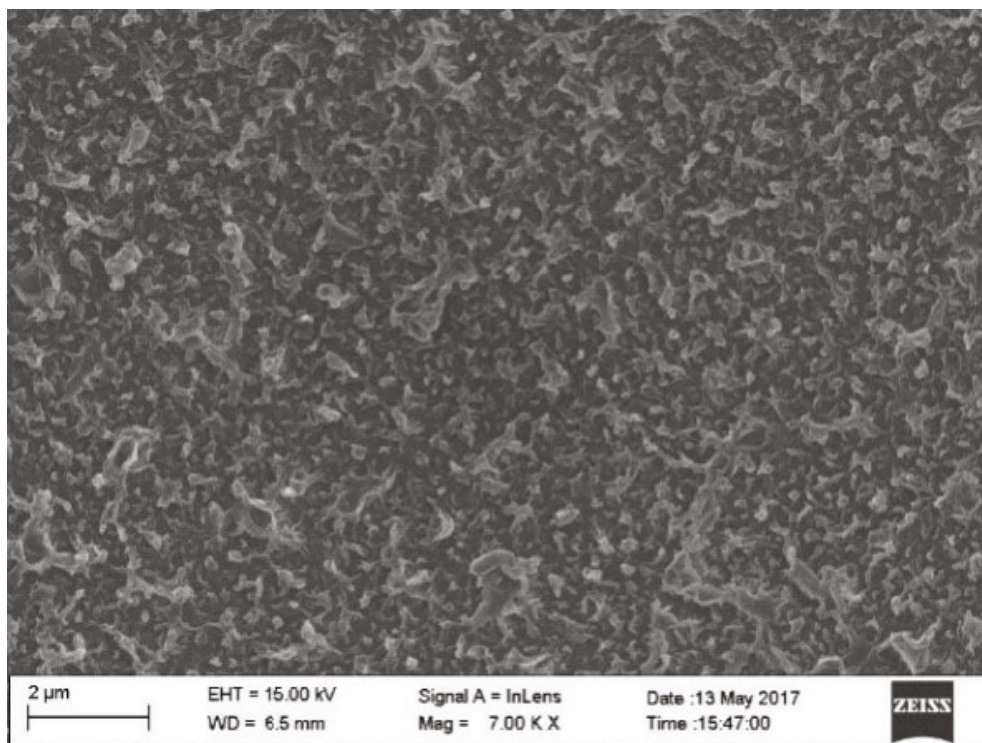
The surface roughness of the 0, 0.004, and 0.008-MG-TFN membranes was measured using an atomic force microscope (AFM, MultiMode 8, Bruker, Germany). The samples

of membranes were dried out and cut into pieces; then, they are fixed on the sample table with double-sided tape.
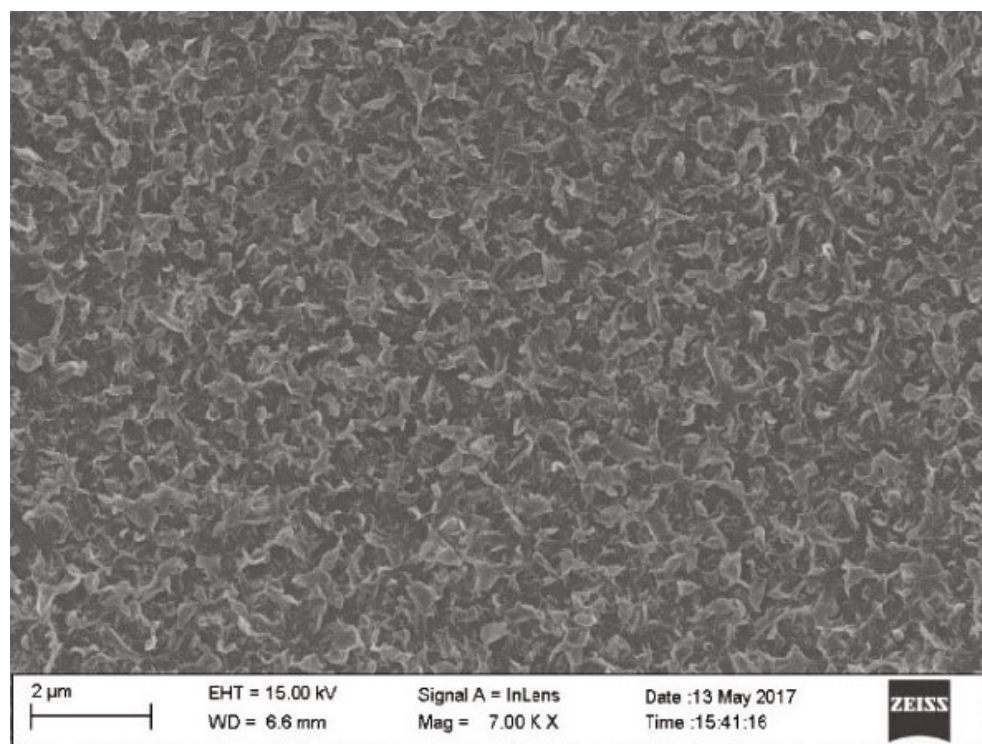
The surface morphologies of the 0, 0.004, and 0.008-MG-TFN membranes were examined using a scanning electron microscope (SEM, SIGMA, ZEISS, Germany) to determine the change in the ridge and valley structure with different concentrations of MG. The samples of membranes were dried out and cut into pieces; then, they were coated with a platinum sputter coater. The SEM was operated in 15 kV and at 7000 times magnification.

2.4. Performance of MG-TFN Membrane. The membrane perm selectivity of the 0, 0.002, 0.004, 0.006, and 0.008-MG-TFN membranes was evaluated with a lab-scale cross-flow filtration system (FlowMem-0021-HP, Xiamen Filter, China). A 2 g/L NaCl aqueous solution flowed in the cross-flow module and the temperature was maintained at 25°C using a low-temperature bath circulator (DLSB-10/20, Zhengzhou Great Wall, China). Prefiltration was conducted at 1.5 MPa for 10 min to achieve membrane compaction before the main filtration, which was performed at 1.5 MPa for 30 min. At the end of the run, both the water flux and the salt rejection were measured.

The antifouling performance of the TFC and MG-TFN membranes was also evaluated using the cross-flow filtration system described above. The membranes were first prepressurized in a 2 g/L sodium chloride solution for 50 minutes to measure the stable water flux through the membranes, then replaced with a feed solution of 1 g/L BSA, which was used to simulate the foul filtration conditions in the presence of contaminants. After 80 minutes of operation, the device was cleaned with pure water for half an hour. The above steps

| 2 μm | EHT = 15.00 kV | Signal A = InLens | Date :13 May 2017 | ZEISS |
| | WD = 6.5 mm | Mag = 7.00 K X | Time :15:47:00 | |

(a)

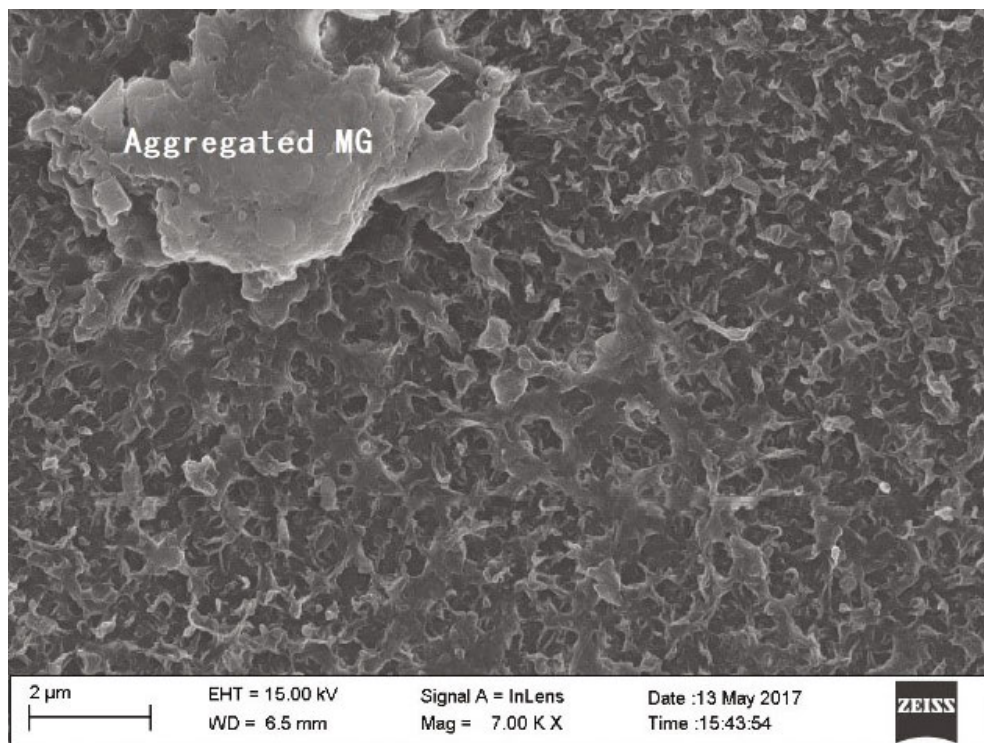| 2 μm | EHT = 15.00 kV | Signal A = InLens | Date :13 May 2017 | ZEISS |
| | WD = 6.6 mm | Mag = 7.00 K X | Time :15:41:16 | |

(b)

Figure 4: Continued.

(c)

FIGURE 4: SEM images of the top surfaces of composite membranes prepared with different MG concentrations: (a) 0 wt%, (b) 0.004 wt%, and (c) 0.008 wt%.

were repeated to determine the flux return rate after contamination. The pressure was kept constant at 1.5 MPa during the experiment.

3. Results and Discussion

3.1. Characterization of MG-TFN Membrane. The results of the FTIR analysis of the TFC and MG-TFN membranes are shown in Figure 1. The FTIR spectra indicate the presence of O-H groups (3302 cm^{-1}), C=O stretching vibration in amino groups (1648 cm^{-1}), N-H deformation vibration in amino groups (1613 cm^{-1}), and O-H deformation vibration in carboxyl groups (1417 cm^{-1}). Compared with the TFC membrane without MG, the band intensity of C=O and N-H in amino groups is lower in the 0.004 and 0.008-MG-TFN membrane. The band of C=O shifts to 1658 cm^{-1} in the 0.004-MG-TFN membrane and to 1661 cm^{-1} in the 0.008-MG-TFN membrane. Meanwhile, the intensity of O-H stretching vibration (3302 cm^{-1}) becomes stronger with the increasing of the concentration of MG. The above analysis reveals that the addition of MG could change the band shift and band intensity of the composite membrane, especially between 500 cm^{-1} and 1700 cm^{-1}, which indicates the interaction between the MG and the PA active layer.

The water contact angles of membrane surfaces under different MG incorporating concentrations are shown in Figure 2. When MG is added into the water phase of interfacial polymerization, the hydrophilicity of the composite membrane surface is affected to some extent. Hydrophilicity is expressed by the contact angle of water on the membrane surface. A smaller water contact angle means a better hydrophilicity of the membrane. It can be seen from the figure that with the increase of MG concentration from 0 to 0.008 wt%, the contact angle decreases from 37.7 to 32.2, which indicates that the hydrophilicity of the membrane surface increases after adding MG. This is because MG has abundant hydrophilic groups (carboxyl, hydroxyl, and epoxy groups) on its surface. The hydrophilic membrane surface will promote water molecules to transport to the membrane surface, thus increasing water permeability.

As shown in Figure 3, it could be observed that MG incorporation could change the surface roughness of the membranes from the AFM images of top views of the 0, 0.004, and 0.008-MG-TFN membranes. Quantitative information such as arithmetic mean roughness (Ra) and root mean square roughness (Rq) of the selected district of the AFM images was obtained using NanoScope Analysis. The surface roughness of the blank control TFC membrane is the smallest with an Rq of 30.4. When the MG concentration is 0.004 wt%, the TFN membrane has the largest surface roughness with an Rq of 98.1. However, when the MG concentration increases to 0.008 wt%, the surface roughness of the TFN membrane decreases to 73.4.

As shown in Figure 4, the SEM images of TFC and TFN membranes reflect the different surface morphological details. It could be observed that all the membrane surfaces are rough and have staggered structure with ridge and valley, which is the typical structural feature of PA-TFC. Compared with the TFC membrane without MG, the membrane surfaces of the MG-TFN membranes are rougher with
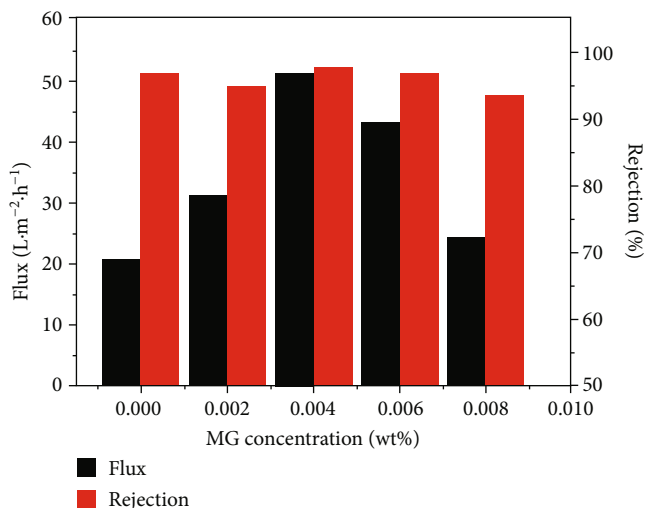
FIGURE 5: Water flux and rejection of membranes prepared with different MG concentrations.

increased cross-linking, which is in agreement with the results of AFM. When the MG concentration incorporating in the aqueous phase is 0.008 wt%, aggregated MG nanosheets could be observed in the TFN membrane surface.

3.2. Performance of MG-TFN Membrane. Figure 5 shows the effect of the MG doping concentration on the water flux and rejection of the prepared TFN membranes. As can be seen from the figure, with the MG concentration increase, the water flux of the RO TFN membrane increases first and then decreases, while the rejection is basically unchanged. When the concentration of MG is 0.004 wt%, the maximum water flux of the TFN membrane reaches 51.0 L m^{-2} h^{-1} and the rejection of NaCl is 97.5%. Compared with the TFC membrane, the water flux of the MG-TFN membrane is greatly increased by about 1.5 times (51.0 L m^{-2} h^{-1} vs. 20.6 L m^{-2} h^{-1}), and the rejection of NaCl remains at a high level (97.5% vs. 96.6%). The reasons for the water flux increase of the MG-TFN membrane may include as follows.

On the one side, water molecules can pass through the unique nanolayers of MG. On the other hand, the surface of MG contains a large number of hydrophilic groups (hydroxyl, carboxyl, and epoxy groups). The hydrophilic membrane surface causes water molecules to transport to the membrane surface, thus increasing the permeability of water. Furthermore, the surface roughness of the membrane increases, and the effective area of the membrane brings the membrane in contact with more water molecules. However, the membrane surface thickness also affects water flux, and the addition of a low concentration of MG to the water phase system may help to form a thin PA active layer, thus improving the water permeability of the TFN membrane. Nevertheless, an increase in the surface thickness of the composite membrane occurs when incorporating high concentrations of MG, which increases the resistance of water passage The above factors have little effect on the rejection of salt ions, so the NaCl rejection of the MG-TFN membrane could be maintained at a certain level. Therefore, the incor-
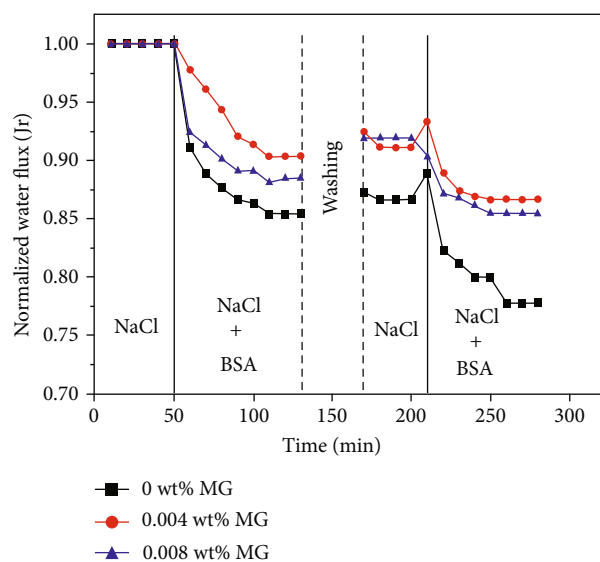

FIGURE 6: A comparison of flux recoveries for the composite membranes prepared with different MG concentrations.

poration of MG can significantly increase the water flux of the membrane while maintaining a high salt rejection.

Figure 6 shows the normalized water flux curve with time of the TFC and MG-TFN membranes in the antifouling test. According to the figure, the flux of all membranes is reduced after the pollution process. The membrane flux can recover to a certain level after washing with pure water, but it could not be fully recovered. However, the MG-TFN membranes show a higher antifouling performance. The 0.004-MG-TFN membrane flux recovers by 91.1%, while the TFC membrane flux recovery only reaches to 86.6%. The improved antifouling performance of MG-TFN membrane may be attributed to the improved hydrophilicity of the membrane caused by MG incorporation. Since the BSA is negatively charged at pH 7, electrostatic interactions occur

between the membrane surface and the contaminant BSA, resulting in less contamination of the TFN membrane.

4. Conclusions

MG-TFN membranes were successfully prepared by dispersing MG into the MPD solution. It could be deduced from FTIR that MG bound well to the PA layer. SEM and AFM results confirm that the MG incorporation results in the change of surface roughness of the TFN membrane, and the 0.004-MG-TFN membrane has the highest surface roughness. The higher MG incorporation concentration leads to the aggregation of MG and the reduction of roughness, which is negative for the membrane performance. The introduction of MG also leads to an increase in membrane hydrophilicity. The MG-TFN membrane exhibits better separation performance and stronger antifouling performance compared to the TFC membrane. The optimal 0.004-MG-TFN membrane reaches a flux of $51 \, L \, m^{-2} \cdot h^{-1}$, which is 1.5 times higher than that of the TFC membrane, while maintaining a high NaCl rejection of 97.5%.

Data Availability

The data used to support the findings of this study are available from the corresponding author upon request.

Conflicts of Interest

The authors declare that they have no conflict of interest.

References

[1] Z. B. Wang, Z. W. Yang, X. L. Xing, C. X. Gao, L. Y. Chu, and W. M. Chen, "Development and application of membrane separation technology," *Journal of Filtration & Separation*, vol. 18, no. 2, pp. 19–36, 2008.

[2] Z. X. Yue, D. Z. Ma, L. N. Zhao, and H. M. Zhao, "Application and development trend of membrane separation technique," *Yunnan Geographic Environment Research*, vol. 18, no. 5, pp. 52–57, 2006.

[3] J. P. Yang and Q. X. Xiang, "Preparation method and research progress of polymer membrane materials," *Technology wind*, vol. 1, pp. 82–85, 2016.

[4] G. Q. Ni, T. Xie, H. Hu, J. Zhu, and Y. F. Sui, "Application of reverse osmosis technology in water treatment," *Technology & Development of Chemical Industry*, vol. 41, no. 10, pp. 23–27, 2012.

[5] J. Xu, Z. Wang, J. X. Wang, and S. C. Wang, "Progress in the development and application of reverse osmosis membrane technology," *Chemical Industry and Engineering*, vol. 27, no. 4, pp. 351–357, 2010.

[6] G. D. Li, W. Wang, F. J. Li, Q. Ren, and H. Su, "Development of hollow fiber reverse osmosis membrane," *Polymer Bulletin*, vol. 7, pp. 37–42, 2010.

[7] T. Y. Liu, Y. Y. Fang, and X. L. Wang, "Current status and prospect of reverse osmosis membrane materials for desalination," *New Materials Industry*, vol. 5, pp. 1–6, 2012.

[8] Z. H. Wang, H. R. Yu, J. F. Xia et al., "Novel GO-blended PVDF ultrafiltration membranes," *Desalination*, vol. 299, no. 8, pp. 50–54, 2012.

[9] B. X. Mi, "Graphene oxide membranes for ionic and molecular sieving," *Science*, vol. 343, no. 6172, pp. 740–742, 2014.

[10] P. Z. Sun, Q. Chen, X. D. Li et al., "Highly efficient quasi-static water desalination using monolayer graphene oxide/titania hybrid laminates," *NPG Asia Materials*, vol. 7, no. 2, p. e162, 2015.

[11] Y. Lu, H. Y. Zhao, L. Zhang, and L. A. Hou, "Preparation and characterization of mixed matrix RO membrane of polyamide and GO," *Strategic Study of CAE*, vol. 16, no. 7, pp. 84–88, 2014.

[12] M. Y. Wang, *Modification study of carbon fiber/BMI composites by functionalized graphene*, Shenyang University of Aerospace Science and Astronautics, Shenyang, 2016.